

# CAE-P: COMPRESSIVE AUTOENCODER WITH PRUNING BASED ON ADMM

Haimeng Zhao

Shanghai High School  
Shanghai, China

## ABSTRACT

TODO

**Index Terms**— autoencoder, lossy image compression, neural network pruning

## 1. INTRODUCTION

After compressive autoencoder (CAE) was proposed by Theis et al.[2], autoencoder, as a simple and efficient neural network model, has achieved better performance than traditional codecs such as JPEG[3], JPEG 2000[4] etc. This way of lossy image compression can adaptably learn the features of target images and therefore outperforms other codecs.

The main problem a CAE needs to solve is the so-called rate-distortion tradeoff, which is the balance between the distortion of the reconstructed image and the original image and the bitrate. The problem can be paraphrased as the following:

$$\min_{E,D} d + \beta R,$$

where  $d$  stands for the distortion,  $R$  represents the bitrate and  $\beta > 0$  controls the balance.

TODO

## 2. RELATED WORK

Lossy image compression methods based on deep neural networks have provoked extensive attention due to their potential on learning better presentations. One of the commonly used network structures is the compressive autoencoder (CAE)[5][2][6][7][8], an convolutional autoencoder targetted at minimizing  $d + \beta R$ . MSE (Mean-Squared Error), SSIM and MS-SSIM are the most widely used metrics for  $d$  while  $R$  is often approximated by  $H$  learned by an extra entropy estimator, in the form of an generative model[6], GMS[2], context models[9] etc. Other deep lossy image compression methods include GAN[10], GDN (Generalized Divisive Normalization)[6] and RNN[11][1].

The ADMM pruning method we introduced is inspired by the field of neural network architecture search. Han et al. first

Thanks to SJTU Student Innovation Center for providing GPU resources.

proposed the pruning method in 2015[12]. Many improvements have been put forward later on[13][14][15][16][17]. Zhang et al. proposed an systematic pruning method and provided with a theoretical explanation based on ADMM for it[18][19]. Adversarial learning and genetic algorithms are other architecture searching methods.

## 3. PROPOSED METHOD

A basic compressive autoencoder (CAE), consisting of an encoder  $E$ , a decoder  $D$  and a quantizer  $Q$  as proposed by Theis et al.[2], is defined as follows:

$$\begin{aligned} E : \mathbb{R}^n &\rightarrow \mathbb{R}^m, \\ D : \mathbb{R}^m &\rightarrow \mathbb{R}^n, \\ Q : \mathbb{R} &\rightarrow \mathbb{Z}. \end{aligned}$$

The encoder  $E$  maps the original image  $\mathbf{x}$  to a latent representation  $\mathbf{z} := E(\mathbf{x})$ . The quantizer  $Q$  then maps each element of  $\mathbf{z}$  to  $\mathbb{Z}$ , which produces the quantized and compressed code of the image  $\hat{\mathbf{z}} := Q(\mathbf{z})$ . And the decoder  $D$  tries to reconstruct the original image  $\hat{\mathbf{x}} := D(\hat{\mathbf{z}})$  from the code  $\hat{\mathbf{z}}$ .

Our aim is to let the reconstructed image  $\hat{\mathbf{x}}$  looks as similar as the original image  $\mathbf{x}$ , and at the same time, reduce the number of bits needed to store the code, or bitrate  $R$ . The problem in question can be paraphrased as:

$$\min_{E,D} d(\mathbf{x}, \hat{\mathbf{x}}) + \beta R(\hat{\mathbf{z}}).$$

In the following subsections, we will explain in detail how to select the appropriate encoder  $E$ , decoder  $D$  and quantizer  $Q$  and how to solve the optimization problem mentioned above.

### 3.1. Selection of $E$ , $D$ and $Q$

Similar to the original CAE, we choose convolutional layers to be the basis of our encoder and decoder, which forms a convolutional autoencoder. To avoid problems such as gradient vanishing, we select residual blocks as the building unit of our autoencoder. The decoder mirrors the structure of the encoder to maintain symmetry, except that it replaces the downsampling convolutional layers with sub-pixel convolutional layers proposed by Shi et al.[20] to perform upsampling.

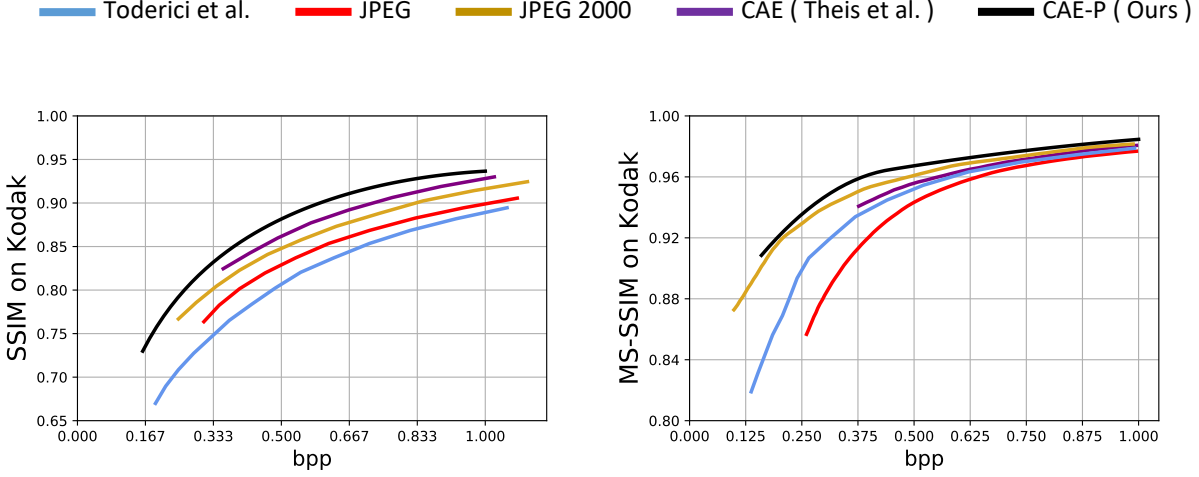


**Fig. 1.** Comparison of different method with respect to SSIM and MS-SSIM on the Kodak PhotoCD dataset. Note that Toderici et al.[1] used RNN structure instead of entropy coding while CAE-P (Ours) replaces entropy coding with pruning method.

It should be noted that convolutional layers in the autoencoder can learn a set of feature maps from data, and the pruning method we are going to introduce in section 3.2 actually urges the autoencoder to abandon those unimportant features while those essential features are retained.

Various kinds of quantizers have been developed so far. We choose to use a simple and computational friendly one proposed by Theis et al.[2] who was inspired by the random binary quantizer developed by Toderici et al.[11]. It is defined as:

$$Q(t) := \lfloor t \rfloor + \epsilon, \epsilon \in \{0, 1\},$$

in which  $\epsilon$  plays the role of a switch deciding whether to output the ground or the ceiling of the input number, and the probability of  $\epsilon = 1$  satisfies  $P(\epsilon = 1) = t - \lfloor t \rfloor$ . To make the quantizer differentiable, we replace its gradient with its expectation:

$$\frac{\partial}{\partial t} Q(t) := \frac{\partial}{\partial t} \mathbb{E}[Q(t)] = \frac{\partial}{\partial t} t = 1$$

### 3.2. Solution to the optimization problem

In order to furtherer reformulate the optimization problem mentioned in Section 3, we must carefully select appropriate metrics for both  $d(\mathbf{x}, \hat{\mathbf{x}})$  and  $R$ .

MSE, SSIM and MS-SSIM are the most commonly used metrics for  $d(\mathbf{x}, \hat{\mathbf{x}})$ , while  $R$  is approximated by the entropy of the latent code  $\mathbf{z}$  due to its discreteness in the existing research which often requires extra efforts in building a proper entropy

estimator. We here introduce a pruning approach to solve this problem more straightforward and more accurate.

First, we can reformulate  $R$  by

$$R(\hat{\mathbf{z}}) = \text{card}(\hat{\mathbf{z}}) = \text{card}(\mathbf{z}) = \text{card}(E(\mathbf{x})),$$

in which  $\text{card}(\cdot)$  counts the number of non-zero elements. If we want  $\mathbf{z}$  generated by the encoder to have fewer number of non-zero elements than a desired number  $\ell$ , we can rephrase the problem into an ADMM(Alternating Direction Method of Multipliers)-solvable problem inspired by Ye et al.[19]:

$$\begin{aligned} & \min_{E, D} d(\mathbf{x}, \hat{\mathbf{x}}) + g(\mathbf{Z}), \\ & \text{s.t. } E(\mathbf{x}) - \mathbf{Z} = 0. \end{aligned}$$

where the indicator function  $g(\cdot)$  is defined as

$$g(\mathbf{Z}) := \begin{cases} 0 & \text{if } \text{card}(\mathbf{Z}) \leq \ell, \\ +\infty & \text{otherwise.} \end{cases}$$

By introducing the dual variable  $\mathbf{U}$  and a peanalty factor  $\rho > 0$  we can split the above problem into two sub-problems. The first sub-problem is:

$$\min_{E, D} d(\mathbf{x}, \hat{\mathbf{x}}) + \frac{\rho}{2} \|E(\mathbf{x}) - \mathbf{Z}^k + \mathbf{U}^k\|_F^2,$$

in which  $k$  is the current iteration number and  $\|\cdot\|_F^2$  is the Frobenius norm. This time, the target function is nothing more than a trivial target function plus a  $L_2$  regularization

term, which can be easily solved by back propagation and gradient descent. The second sub-problem is:

$$\min_{\mathbf{Z}} g(\mathbf{Z}) + \frac{\rho}{2} \|E^{k+1}(\mathbf{x}) - \mathbf{Z} + \mathbf{U}^k\|_F^2.$$

The solution to this problem was derived by Boyd et al. in 2011[21]:

$$\mathbf{Z}^{k+1} = \Pi_{\mathbf{S}}(E^{k+1}(\mathbf{x}) + \mathbf{U}^k),$$

where  $\mathbf{S} = \{E \mid \text{card}(E(\mathbf{x})) \leq \ell\}$  and  $\Pi_{\mathbf{S}}(\cdot)$  represents the Euclidean projection onto the set  $\mathbf{S}$ . Generally, Euclidean projection onto a nonconvex set is difficult, but Boyd et al.[21] have proved that the optimal solution is to keep the  $\ell$  largest elements of  $E^{k+1}(\mathbf{x}) + \mathbf{U}^k$  and set the rest to zero. Finally, we will update the dual variable  $\mathbf{U}$  with the following policy:

$$\mathbf{U}^{k+1} = \mathbf{U}^k + E^{k+1}(\mathbf{x}) - \mathbf{Z}^{k+1}.$$

These three steps together form one iteration of the ADMM pruning method. The complete algorithm is shown in Algorithm 1.

---

#### Algorithm 1 Pruning of $E(\mathbf{x})$ Based on ADMM

---

##### Input:

$\mathbf{x}$ : A batch of input images;  
 $E, D$ : The encoder and decoder;  
 $\ell$ : The expected number of non-zero elements in  $E(\mathbf{x})$ ;  
 $k_m$ : Max number of iterations.

##### Output:

$E, D$ : Trained encoder and decoder;  
 $\mathbf{U}, \mathbf{Z} \Leftarrow$  zeroes with the same shape as  $E(\mathbf{x})$   
**for**  $1 \leq k \leq k_m$  **do**  
 $E, D \Leftarrow \arg \min_{E, D} d(\mathbf{x}, \hat{\mathbf{x}}) + \frac{\rho}{2} \|E(\mathbf{x}) - \mathbf{Z} + \mathbf{U}\|_F^2$ ;  
 $\mathbf{Z} \Leftarrow$  keep the  $\ell$  largest elements in  $E(\mathbf{x}) + \mathbf{U}$  and set the rest to 0;  
 $\mathbf{U} \Leftarrow \mathbf{U} + E(\mathbf{x}) - \mathbf{Z}$ .  
**end for**  
**return**  $E, D$

---

Note that the ADMM algorithm cannot assure that the final number of non-zero elements is strictly less than  $\ell$ . Actually, at convergence, there will be many zero-close elements that are not exactly zero. But our quantizer will remedy it by rounding them down to zero.

## 4. EXPERIMENT

### 4.1. Model architecture

Our method is a direct modification of CAE proposed by Theis et al.[2]. The encoder and decoder are composed of convolutional layers as described in Section 3.1. The input image is first downsampled by three convolutional blocks each containing a convolutional layer, a batch normalization

layer and a PReLU layer. Following 15 residual blocks, two more downsampling convolutional blocks and the last convolutional block for fine-tune are applied, generating  $\mathbf{z}$ . It is then quantized by the quantizer  $Q$  and inputted into the decoder whose architecture mirrors the encoder.

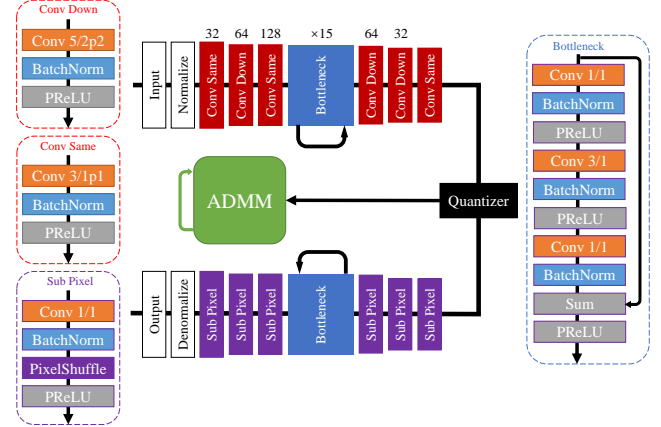


**Fig. 2.** The architecture of CAE-P. “Conv k/spP” stands for a convolutional layer with kernel size  $k \times k$  with a stride of  $s$  and a reflection padding of  $P$ . “Conv Down” means reducing the height and weight by 2 and “Conv Same” means maintaining them. The residual block “Bottleneck” is repeated 15 times in a row. The decoder mirrors the architecture of the encoder.

### 4.2. Training

We use the Adam optimizer [22] with batch size set to 32 to solve the first sub-problem mentioned in Section 3.2. Learning rate is set to  $4 \cdot 10^{-3}$  and decreases as the training procedure proceed: halved each time the loss has not dropped for 10 epochs. Every 20 epochs, the second and third steps of the ADMM pruning method is applied. The ratio of the number of elements to retain in step two is set to be 10%. For models of different bpp, we modify the last layer of the encoder to fine tune. All codes are implemented in PyTorch and open-sourced<sup>1</sup>. Each model is trained for 300 epochs on 4 GPUs.

### 4.3. Datasets and preprocessing

We use BSDS500[23] as the training set which contains five hundred  $481 \times 321$  natural images. The images are randomly cropped to  $128 \times 128$ , horizontally and vertically flipped and then normalized. As for the test set, we select the commonly used Kodak PhotoCD dataset<sup>2</sup>, which contains twenty-four  $768 \times 512$  images.

<sup>1</sup><https://github.com/JasonZHM/CAEP>

<sup>2</sup><http://r0k.us/graphics/kodak/>

#### 4.4. Results and discussion

We tested CAE-P (Our method), JPEG (implemented by libjpeg<sup>3</sup>) and JPEG 2000 (implemented by Kadadu Software<sup>4</sup>) on Kodak PhotoCD dataset. We used the open-source implementation of SSIM & MS-SSIM<sup>5</sup>. Since different methods under high bpp segment show similar performance, different from the bpp range [0, 3] selected by the previous work, we used [0, 1] instead to better distinguish different methods. In both metrics, the performance of each method on Kodak under different bpp is averaged, which generated three curves each on the bpp-SSIM/MS-SSIM plane. We digitized the Kodak curve from the paper of Theis et al.[2] due to the unavailability of their code.

Fig. 1 shows a comparison of the performance achieved by the mentioned methods on Kodak. Our method (CAE-P) outperforms all the other methods in both SSIM and MS-SSIM, especially the original CAE which uses entropy coding. Note that the blue curve represents the RNN-based method proposed by Toderici et al. which does not include a entropy estimator. Having replaced entropy coding with ADMM pruning method, CAE-P outperforms both entropy coding models and RNN-based methods. Thus, the effectiveness of our pruning method is proved.

In Fig. 3, we exhibited the actual compression renderings of different methods visually: the origin (top left), JPEG (top right), CAE-P (ours, bottom left) and JPEG 2000 (bottom right). As can be noticed, JPEG breaks down under a bpp of 0.3 while CAE-P’s and JPEG’s are still perpetually acceptable. The color of the rocks appears slightly greener in CAE-P’s output, which may well be the consequence of the selection of perpetual metric used during training. Focus on the middle right region containing clouds. CAE-P handles soft structures such as clouds and water ripples better than the others. More visual examples under different bpps are available along with the source code on github.

Model	bpp	ratio of zeros
Before pruning	1.422	9.60%
After pruning	1.012	21.51%
Variation	-28.83%	+124.1%

**Table 1.** Bpp & ratio of zeros (number of zero elements in  $\hat{z}$  divided by the total number of elements in  $\hat{z}$ ) before and after pruning. The structures of  $E$  &  $D$  are preserved.

To better illustrate the effectiveness of the ADMM pruning method we introduced, we first trained a model without pruning and then apply pruning method to it. As listed in Table 1, the bpp is decreased by 28.83% and the ratio of zeros in  $\hat{z}$  is increased by 124.1% after pruning. By simple calculations, we can see that the number of non-zero elements in  $\hat{z}$

has been cut down by -13.18%.



**Fig. 3.** Performance of different methods on kodim21 from Kodak dataset. Bpp is set to be about 0.3.

## 5. CONCLUSION

In this paper, we proposed the compressive autoencoder with pruning based on ADMM (CAE-P) which replaces the traditionally used entropy estimating technique in deep-learning-based lossy image compression with ADMM pruning method inspired by the field of neural network architecture search and avoided the extra effort needed for training an entropy estimator. We tested our models on natural images and achieved better results than the original CAE model which relies on entropy coding along with other mentioned methods. We further explored the effectiveness of the ADMM-based pruning method in CAE-P by looking into the detail of latent codes learned by the model.

Further study can focus on developing and applying more efficient and delicate pruning method to deep lossy image compression systems rather than our simple pruning method. Also, the structures of  $E$ ,  $D$  and  $Q$  are worth studying.

## 6. REFERENCES

- [1] George Toderici, Damien Vincent, Nick Johnston, Sung Jin Hwang, David Minnen, Joel Shor, and Michele Covell, “Full resolution image compression with recurrent neural networks.,” in *CVPR*, 2017, pp. 5435–5443.
- [2] Lucas Theis, Wenzhe Shi, Andrew Cunningham, and Ferenc Huszár, “Lossy image compression with compressive autoencoders,” *arXiv preprint arXiv:1703.00395*, 2017.

<sup>3</sup><http://libjpeg.sourceforge.net/>

<sup>4</sup><http://kakadusoftware.com/>

<sup>5</sup><https://github.com/jorge-pessoa/pytorch-msssim>

- [3] Gregory K Wallace, “The jpeg still picture compression standard,” *IEEE transactions on consumer electronics*, vol. 38, no. 1, pp. xviii–xxxiv, 1992.
- [4] David S. Taubman and Michael W. Marcellin, *JPEG 2000: Image Compression Fundamentals, Standards and Practice*, 2002.
- [5] Feng Jiang, Wen Tao, Shaohui Liu, Jie Ren, Xun Guo, and Debin Zhao, “An end-to-end compression framework based on convolutional neural networks,” *IEEE Transactions on Circuits and Systems for Video Technology*, 2017.
- [6] Johannes Ballé, Valero Laparra, and Eero P Simoncelli, “End-to-end optimization of nonlinear transform codes for perceptual quality,” in *Picture Coding Symposium (PCS), 2016*. IEEE, 2016, pp. 1–5.
- [7] Eirikur Agustsson, Fabian Mentzer, Michael Tschanen, Lukas Cavigelli, Radu Timofte, Luca Benini, and Luc V Gool, “Soft-to-hard vector quantization for end-to-end learning compressible representations,” in *Advances in Neural Information Processing Systems*, 2017, pp. 1141–1151.
- [8] Mu Li, Wangmeng Zuo, Shuhang Gu, Debin Zhao, and David Zhang, “Learning convolutional networks for content-weighted image compression,” *arXiv preprint arXiv:1703.10553*, 2017.
- [9] Fabian Mentzer, Eirikur Agustsson, Michael Tschanen, Radu Timofte, and Luc Van Gool, “Conditional probability models for deep image compression,” in *IEEE Conference on Computer Vision and Pattern Recognition (CVPR)*, 2018, vol. 1, p. 3.
- [10] Oren Rippel and Lubomir Bourdev, “Real-time adaptive image compression,” *arXiv preprint arXiv:1705.05823*, 2017.
- [11] George Toderici, Sean M O’Malley, Sung Jin Hwang, Damien Vincent, David Minnen, Shumeet Baluja, Michele Covell, and Rahul Sukthankar, “Variable rate image compression with recurrent neural networks,” *arXiv preprint arXiv:1511.06085*, 2015.
- [12] Song Han, Jeff Pool, John Tran, and William Dally, “Learning both weights and connections for efficient neural network,” in *Advances in neural information processing systems*, 2015, pp. 1135–1143.
- [13] Tien Ju Yang, Yu Hsin Chen, and Vivienne Sze, “Designing energy-efficient convolutional neural networks using energy-aware pruning,” pp. 6071–6079, 2017.
- [14] Yiwen Guo, Anbang Yao, and Yurong Chen, “Dynamic network surgery for efficient dnns,” vol. to appear, 2016.
- [15] Xiaoliang Dai, Hongxu Yin, and Niraj K Jha, “Nest: A neural network synthesis tool based on a grow-and-prune paradigm,” *arXiv preprint arXiv:1711.02017*, 2017.
- [16] Wei Wen, Chunpeng Wu, Yandan Wang, Yiran Chen, and Hai Li, “Learning structured sparsity in deep neural networks,” 2016.
- [17] Yihui He, Xiangyu Zhang, and Jian Sun, “Channel pruning for accelerating very deep neural networks,” 2017.
- [18] Tianyun Zhang, Shaokai Ye, Kaiqi Zhang, Jian Tang, Wujie Wen, Makan Fardad, and Yanzhi Wang, “A systematic dnn weight pruning framework using alternating direction method of multipliers,” *arXiv preprint arXiv:1804.03294*, 2018.
- [19] Shaokai Ye, Tianyun Zhang, Kaiqi Zhang, Jiayu Li, Kaidi Xu, Yunfei Yang, Fuxun Yu, Jian Tang, Makan Fardad, Sijia Liu, et al., “Progressive weight pruning of deep neural networks using admm,” *arXiv preprint arXiv:1810.07378*, 2018.
- [20] Wenzhe Shi, Jose Caballero, Ferenc Huszar, Johannes Totz, Andrew P. Aitken, Rob Bishop, Daniel Rueckert, and Zehan Wang, “Real-time single image and video super-resolution using an efficient sub-pixel convolutional neural network,” pp. 1874–1883, 2016.
- [21] Stephen Boyd, Neal Parikh, Eric Chu, Borja Peleato, and Jonathan Eckstein, “Distributed optimization and statistical learning via the alternating direction method of multipliers,” *Foundations & Trends in Machine Learning*, vol. 3, no. 1, pp. 1–122, 2011.
- [22] Diederik P Kingma and Jimmy Ba, “Adam: A method for stochastic optimization,” *arXiv preprint arXiv:1412.6980*, 2014.
- [23] David Martin, Charless Fowlkes, Doron Tal, and Jitendra Malik, “A database of human segmented natural images and its application to evaluating segmentation algorithms and measuring ecological statistics,” in *Computer Vision, 2001. ICCV 2001. Proceedings. Eighth IEEE International Conference on*. IEEE, 2001, vol. 2, pp. 416–423.